Wang Y, et al. Iran J Immunol. 2019; 16(4):278-290.
https://doi.org/10.22034/iji.2019.80279.

Iranian Journal of Immunology (IJI)
iji@sums.ac.ir

ORIGINAL ARTICLE

Multiple Myeloma Bone Marrow Mesenchymal Stromal Cells Inhibit CD8$^+$ T Cell Function in a Process that May Implicate Fibroblast Activation Protein α

Yadan Wang[1†], Xiaofei Wu[2†], Yu Hu[1*]

[1]Department of Hematology, Institute of Hematology, Union Hospital, Tongji Medical College, Huazhong University of Science and Technology, [2]Institute of Hematology, The Central Hospital of Wuhan, Tongji Medical College, Huazhong University of Science and Technology, Wuhan, Hubei, China

ABSTRACT

Background: Multiple myeloma (MM) is a malignant plasma cell proliferative disorder with limited immunotherapy treatment because of T cell dysfunction. **Objective:** To investigate the immunomodulatory function of bone marrow mesenchymal stromal cells (MM-BMSCs) on CD8$^+$ T cells. **Methods:** Proliferation and cytotoxicity were detected by cell counting kit-8 assay. Cell cycle was detected by flow cytometry, and p16 expression was detected by PCR. The expression of fibroblast activation protein α (FAPα) was evaluated by immunohistochemistry. **Results:** Co-culture of CD8$^+$ T cells with MM-BMSCs decreased the cell survival rate and increased the killing rate ($p=0.03$, $p=0.001$, respectively), the percentage of cells in G0/G1 phase and p16 expression ($p<0.001$). FAPα was mainly in the mesenchymal matrix of the MM microenvironment and elevated in MM derived bone marrow compared to healthy donors ($p<0.001$). The FAPα inhibitor PT-100, increased survival and the killing rate ($p<0.001$, $p=0.043$, respectively), and decreased the percentage of cells in G0/G1 phase and p16 expression ($p=0.024$, $p=0.004$, respectively). **Conclusion:** Therefore, MM-BMSCs inhibit the proliferation and cytotoxicity of CD8$^+$ T cells, significantly block the cell cycle and increase p16 expression in co-cultured CD8$^+$ T cells in a cell-cell contact-dependent manner.

Received: 2019-07-29, Revised: 2019-11-27, Accepted: 2019-11-28.
Citation: Wang Y, Wu X, Hu Y. Multiple Myeloma Bone Marrow Mesenchymal Stromal Cells Inhibit CD8$^+$ T Cell Function in a Process that May Involve Fibroblast Activation Protein α. *Iran J Immunol.* 2019; 16(4):278-290. doi: 10.22034/iji.2019.80279.

Keywords: Bone Marrow Mesenchymal Stromal Cells, CD8$^+$ T Cell Anergy, Fibroblast Activation Protein a, Multiple Myeloma

*Corresponding author: Dr. Hu Yu, Department of Hematology, Institute of Hematology, Union Hospital, Tongji Medical College, Huazhong University of Science and Technology, Wuhan, Hubei, China, e-mail: dr_huyu@126.com
†These authors contributed equally to this work.

INTRODUCTION

Multiple myeloma (MM) is a clonal B-cell malignancy that accounts for around 10% of hematologic malignancies (1). Until recently MM was characterized by increased blood calcium level, renal failure, anemia, and bone lesions (CRAB). MM diagnosis is assisted by three biomarkers: abnormal serum-free light chains; 60% or higher plasma cell infiltration of the bone marrow; and two or more focal lesions in the bone or bone marrow (2). With novel drugs and immunotherapy, the 5-y survival rate of MM increased to more than 40% (3). However, the long-term therapeutic benefit of immunotherapy is threatened by impaired T cell function in MM (4). The tumor microenvironment plays an important role in growth and progression of malignancies. Thus, interaction of MM cells, immune cells, endothelial cells, fibroblasts and other cells contributes to carcinogenesis (5). As a component of the tumor microenvironment, cancer-associated fibroblasts (CAFs) recruit more tumor suppressive cells into the tumor rather than cytotoxic T cells and show an immunosuppressive effect by increasing Th2, Th17 and Tregs (6-8). According to current knowledge, bone marrow mesenchymal stromal cells (BMSCs) are one origin of CAFs (9). MM-BMSCs show an impaired immunomodulatory function with attenuated proliferation-inhibiting and apoptosis-promoting effects when co-cultured with $CD4^+$ T cells (10). Cell-contact dependent and independent mechanisms are involved in T-cell proliferation inhibition of BMSCs by programmed death-ligand 1 (PD-L1), interleukin-10 (IL-10), transforming growth factor-beta (TGF-β) and prostaglandin E2 (PGE2) (10-12). BMSCs can inhibit the proliferation of both $CD4^+$ and $CD8^+$ activated T cells (13). Our team have already confirmed that MM-BMSCs mainly induce $CD4^+$ T-cell senescence and Th17 differentiation through the PI3K/AKT signaling pathway (14), resulting in MM escaping the immune response. However, few studies have investigated the other immunomodulatory functions of MM-BMSCs on $CD8^+$ T cells. The accumulation of senescent T-cells mediated by p16 in certain types of cancers might be utilized by the tumor cells to escape immune surveillance (15-17). A large fraction of naïve $CD8^+$ T cells express high levels of p16 which is responsible for the exit of a significant proportion of $CD8^+$ T cells from the proliferative population, thus limiting their numerical expansion *in vitro* (18). Several studies found p16 levels could be used to identify HIV+ patients with premature immune aging (17,19). We have investigated differences in senescence marker hTERT and β-gal between healthy donor (HD)- and MM-BMSCs co-cultured $CD4^+$ T cells, MM-BMSCs showed significant senescence induction (14). However, the characteristic of $CD8^+$ T cell senescence in MM has not yet been elucidated. Fibroblast activation protein α (FAPα) is a serine protease with gelatinase activity and type I collagenase activity, which is a vital type II transmembrane protein expressed in more than 90% epithelial tumor stromal cells (20). Elevated FAPα is associated with tumor re-growth, recurrence, and poor clinical outcome in endothelial malignancies (21,22). In multiple myeloma, FAPα facilitates MM cell proliferation and drug resistance through the β-catenin pathway and is involved in tumor immunosuppression (23,24). We have demonstrated that MM-BMSCs in a tumor microenvironment express high levels of FAPα and have confirmed immunosuppression on $CD4^+$ T cells (14). But it is still not known whether FAPα can exert the same immunosuppression effect on $CD8^+$ T cells. We hypothesized that FAPα can cause immunosuppression of $CD8^+$ T cells. Therefore, in this study, we investigated the immunomodulatory functions of MM-BMSCs on $CD8^+$ T cells, including

proliferation, cell cycle, cytotoxicity ability, and identify the expression of FAPα in MM biopsy specimen.

MATERIALS AND METHODS

Bone Marrow (BM) Samples. BM samples were obtained from 5 untreated MM patients and 5 age-matched healthy donors in the Wuhan Union Hospital, China. The clinical information of the MM patients is summarized in Table 1. Informed consent was obtained according to procedures approved by the Ethics Committee of Wuhan Union Hospital.

Table 1. Characteristics of the myeloma patients.

Patient	Sex	Age	Clinical stage	Para protein	Karyotype	Bone lesion
1	M	71	IIIB	IgG-LAM	N	YES
2	M	54	IIIA	IgG-KAP	N	YES
3	F	62	IIIA	IgA-LAM	46, XX, 1q+, del(13)(q14)[6]	NO
4	M	53	IA	IgD-LAM	N	NO
5	F	45	IIIA	IgA-KAP	N	YES

M, male; F, female; N, normal. The clinical stage of the patients was evaluated according to Durie/Salmon scale.

Isolation and Culture of MSCs. Mononuclear cells were separated from bone marrow samples obtained from 5 MM patients and 5 healthy donors, respectively, by Ficoll-Paque (TBD, Tianjin, China) gradient centrifugation. BMSCs were cultured in human MSC serum-free medium containing 5% MSC-stimulatory supplements (Premedics, Beijing, China) at 37°C under 5% CO_2. The culture medium was replaced every 3–4 days, MSCs were detached using 0.125% trypsin-0.01% EDTA and passaged at 1:3. Passage 3 MSCs were harvested and utilized for the experiments (supplementary Figure 1).

Isolation, Activation, and Co-culture of $CD8^+$ T-cells. Human peripheral blood cells from healthy donors were obtained from the Wuhan blood donation center, and their use was approved by the Ethics Committee of Wuhan Union Hospital. Mononuclear cells were separated by Ficoll-Paque gradient centrifugation. A $CD8^+$ microbeads kit (Stem Cell, Vancouver, Canada) was used to separate naïve $CD8^+$ T cells. The 90.6% purity was detected by flow cytometry (supplementary figure 2). For cell-cell culture group experiments 12-well plates were coated with 1 μl/mL anti-CD3 functional antibody (BD) at 4°C overnight for $CD8^+$ T cells stimulation. Passage 3–5 BMSCs were detached and suspended in 2×10^5/mL in 12-well plates. 1×10^6 $CD8^+$ T-cells, with or without stimulation, were co-cultured with BMSCs in the 12-well plates. For the transwell group experiments the same procedure was carried out in 0.4 μm 12-well transwell plates (Corning, USA), $CD8^+$ T cells were cultured at the bottom of the transwell plates. The co-culture medium consisted of RPMI 1640 supplemented with 10% FBS and 50 μg/mL IL-2 (Peprotech, Rocky Hill, USA).

Proliferation Assay. $CD8^+$ T cells co-cultured with or without BMSCs were harvested at day 6 by centrifugation at 1000rpm and resuspended in 1 mL 1640 medium. Inactive $CD8^+$ T cells were used as a control. A 100 μL $CD8^+$ T cell suspension was added into

every well in 96-well plates. The activity was evaluated by a CCK-8 Cell Counting Kit (Dojindo, Japan), according to the manufacturer's instruction.

SA-β-gal Staining. 1×10^6 $CD8^+$ T cells co-cultured with or without BMSCs were harvested into tubes on day 3 and fixed with formaldehyde solution. Staining solution was prepared according to the manufacturer's instruction (Lifetech, USA) and added at 0.5 mL for 1×10^6 $CD8^+$ T cells. After incubation at 37℃ overnight, the T cells were observed under an Olympus BX51 microscope, the blue dyed cells were considered senescent.

T-cell Cycle Analysis. $CD8^+$ T cells co-cultured with or without BMSCs were harvested at day 6 by centrifugation at 1000 rpm and resuspended in 70% cold ethanol at 4°C for 30 minutes, washed with PBS for twice, followed by treatment with 400 μg/mL RNAse A for 20 minutes at 37°C, and stained with 3 μg/mL PI at room temperature for 20 minutes. All stained cells were assessed by a fluorescence-activated cell sorting (FACS) Calibur flow cytometer (BD) and the data was analyzed by FlowJo Version 7.6.1 (TreeStar).

Quantitative Real-time PCR Analysis. $CD8^+$ T cells were harvested and resuspended at a density of 1×10^6 cells/mL in 6-well plates. Total RNA extracted from the cells in TRIzol was used to synthesize cDNA by M-MLV Reverse Transcriptase (GeneCopoeia). The cDNA was amplified with the primers listed in Table 2, using β-actin as an endogenous control. The qRT-PCR program for p16 and β-actin was as follows: initial denaturation at 50°C for 2 min and 95°C for 4 min, followed by 40 cycles of 90°C for 30s and 60°C for 30s. The specificity of the primers was verified by the melting curve. The $2^{-\Delta\Delta CT}$ method was used to estimate the relative quantification of p16 in $CD8^+$ T cells.

Table 2. Primers used in the reverse transcriptase-PCR.

Gene	Sequence
p16	sense 5'- GCT TCC TGG ACA CGC TGG TGG T -3'
	antisense 5'- GGC ATC TAT GCG GGC ATG GTT A -3'
β-actin	sense 5'- AGC GAG CAT CCC CCA AAG TT -3'
	anti-sense 5'- GGG CAC GAA GGC TCA TCA TT -3'

Western Blot. $CD8^+$ T cells were lysed with RIPA buffer on ice, and the protein was quantified with a BCA protein assay kit (Tiangen Biotech Co, China), according to the manufacturer's instructions. The total protein extract was separated by 8% sodium dodecyl sulfate-polyacrylamide gel electrophoresis (SDS-PAGE) and transferred to polyvinylidene fluoride (PVDF) membranes. The membranes were blocked with 5% skim milk, incubated with 1:300 rabbit anti-human p16 polyclonal antibody (Santa cruz) overnight at 4°C, washed in Tris-buffered saline Tween-20 buffer (TBST), followed by incubation with HRP-conjugated goat anti-rabbit IgG (MR Biotech, China) for 1 h at room temperature. The immunoreactive protein bands were visualized by chemiluminescence (Tiangen Biotech).

Immunohistochemical Analysis. We used sections of two-micrometer thickness from formalin-fixed paraffin-embedded bone marrow biopsies obtained from MM patients and healthy donors. Antigen recovery was performed by immersing the sections in citric acid buffer (pH=6.0) and heating in a microwave at moderate power for 10-15 minutes.

After cooling in cold water, the slides were washed three times by PBS (pH=7.4). Immersing the slides in 3% hydrogen peroxide solution for 15 minutes at room temperature, then the slides were washed by PBS twice. Then the slides were incubated at 4°C overnight with anti-FAPα polyclonal antibody (Abcam, Hong Kong, China 1:50 dilution). After returning to room temperature, the slides were washed twice and treated with two drops of polymer helper for 30 minutes at 37°C. Then the slides were washed with PBS and incubated with biotinylated anti-goat immunoglobin (Santa Cruz, 1:200 dilution). The slides were washed with PBS and reacted with 3,3 diaminobenzidinetetrahydrochloride hydrogen peroxide (DAB). Then the slides were counterstained with Harris hematoxylin for 30 seconds. After being washed with PBS, the slides were treated with 1% hydrochloric acid. The slides were washed again in running water, dehydrated and covered with coverslips. The images were captured under Olympus BX51 microscope and analyzed by image pro-plus 6.0.

CTL Assay. The U266 cells were kindly provided by Dr Hu (Department of Hematology, Union Hospital Tongji Medical College Huazhong University of Science and Technology, China). 5×10^5/mL U266 cells were frozen at -80°C and recovered at room temperature for 3-5 cycles to obtain U266 antigen suspension. $CD34^+$ cells were separated from mononuclear cells described above using CD34 microbeads kit (Stem Cell, Vancouver, Canada) for dendritic cell induction, as dendritic cells were served as antigen presenting cells. $CD34^+$ cells were resuspended at 2×10^5/mL in 6-well plates, the medium was RPMI 1640 supplemented with 10% FBS, 1000 U/mL GM-CSF (Peprotech, Rocky Hill, USA) and 1000 U/mL IL-4 (Peprotech, Rocky Hill, USA). Half the medium was replaced every 3 days and on day 7, 100 μL U266 antigen suspension was added into the medium. After stimulation with U266 antigen for 24 hours, the adherent cells were harvested and resuspended at 2×10^5/mL in 6-well plates with 2×10^6/mL activated $CD8^+$ T cells for 2 days. 1×10^6 $CD8^+$ T cells were co-cultured with 2×10^5 BMSCs from MM patients or healthy donors respectively for 3 days, another 1×10^6 $CD8^+$ T cells were considered as control. The U266 cells and $CD8^+$ T cells were suspended in RPMI1640 medium at 1×10^5/mL and 1×10^6/mL respectively. 100 μL U266 cell suspension and 100 μL $CD8^+$ T cell suspension were added to 96-well plates, those were incubated at 37°C for 4 hours. The activity was detected with a CCK-8 kit according to the manufacturer's instruction. The CTL killing rate= [1-(ET-E)/T] ×100%. E represented the OD value of effector cells, T represented the OD value of target cells.

FAPα Inhibitor. We used PT-100 (Huiqiao, Shanghai, China) to interfere with the function of FAPα. PT-100 competitively inhibits the dipeptidyl peptidase (DPP) activity of FAP and CD26/DPP-IV, and a high-affinity interaction is observed with the catalytic site due to the formation of a complex between Ser630/624 and the boron of PT-100. Molecular weight of PT-100 is 310.18 g/mol. We dissolved 31 ug PT-100 in 1 ml PBS, making 1 μmol/mL solution. According to cytotoxicity test of PT-100 in $CD8^+$ T cells and BMSCs before (14), l pmol/ml and 0.1 pmol/ml PT-100 were acceptable. One microliter from 1 μmol/ml and 0.1 μmol/ml PT-100 solution were added in co-cultured medium, making the final concentration l pmol/ml and 0.1 pmol/ml.

Statistical Analysis. The Immunohistochemical images were analyzed by image-pro plus 6.0. Statistical analysis was performed with the statistical SPSS v.13.0 software (SPSS Inc., USA). The paired-sample t-test was used to test the probability of significant differences between samples. The results were expressed as the mean ± SD (standard deviation). Statistical significance was defined as $p<0.05$.

RESULTS

BMSCs affected $CD8^+$ T cell proliferation in a cell-cell dependent manner.
The influence of BMSCs on the growth of $CD8^+$ T-cells was investigated by co-culture of the two cell types in direct contact culture and through transwell culture. The results showed that both HD- and MM-BMSCs inhibited $CD8^+$ T-cell proliferation significantly (Figure 1A, p=0.024, p=0.03, respectively) in direct co-culture. However, there was no obvious differences between BMSCs co-cultured $CD8^+$ T cells and activated T cells in the transwell group (Figure 1B, p>0.05), suggesting that BMSCs affect $CD8^+$ T cell proliferation in a cell-cell dependent manner. In addition, MM-BMSCs did not show an impaired inhibitory effect on $CD8^+$ T cell proliferation (Figure 1A).

MM-BMSCs promoted $CD8^+$ T cell senescence.
As senescent cells are characterized by senescence-associated beta-galactosidase (SA-β-gal) expression, we used SA-β-gal kit to label senescent T cells. We observed increased blue dyed cells in MM-BMSCs groups (Figure 1C, p=0.007, p=0.004, respectively). Senescent T cells were increased by more than 10% in the MM-BMSCs co-culture group, compared with the HD-BMSCs group (Figure 1C, 49.3 ± 12.3, 34.9 ± 5.5%, p=0.04), suggesting MM-BMSCs induced $CD8^+$ T cells senescence.

MM-BMSCs induced $CD8^+$ T cell cycle arrest and p16 expression.
The cell cycle was investigated by flow cytometry. The results showed that both HD- and MM-BMSCs induced $CD8^+$ T cell cycle arrest, because the percentage of T cells in G0/G1 phase was increased with HD- and MM-BMSCs (Figure 1D, p<0.001). The MM-BMSCs increased the G0/G1 phase T cells more than HD-BMSCs (Figure 1D, p=0.005). PCR was used to investigate the level of mRNA of the tumor suppressor gene p16. A noticeable increase of p16 mRNA expression was observed in HD- and MM-BMSCs co-cultured $CD8^+$ T cells (Figure 1E, p<0.001). Consecutively, the expression of p16 was apparently higher in MM-BMSC co-cultured T cells (Figure 1E, p=0.002). Investigation at protein level by western blot showed that HD- and MM-BMSCs both increased p16 expression in $CD8^+$ T cells (Figure 1F, p<0.001), similarly MM-BMSCs promoted higher levels of p16 in $CD8^+$ T cells compared to HD-BMSCs (Figure 1F, p=0.003).

MM-BMSCs impaired tumor specific cytotoxicity of $CD8^+$ T cells.
Cytotoxicity of $CD8^+$ T cells towards U266 antigen activated $CD34^+$ cells was analyzed by CTL assay. We found the tumor specific cytotoxicity was reduced by HD- and MM-BMSCs (Figure 1G, p<0.001, p=0.001, respectively). In addition, HD-BMSCs decreased the killing rate of $CD8^+$ T cells dramatically compared to MM-BMSCs (Figure 1G, p=0.032). Apparently, the inhibitory effect on CTL was impaired in MM-BMSCs.

FAPα was expressed in bone marrow mesenchymal matrix.
We have previously documented that MM-BMSCs stimulated by MM microenvironment expressed high levels of FAPα (14), however, the specific origin of FAPα in bone marrow remains to be elucidated. So, we explored the location of FAPα expression in biopsy specimens. As shown in Figure 2A, we identified FAPα expression in the bone marrow mesenchymal matrix from the positively stained yellow area. We used Image-pro plus 6.0 software to estimate the percentage of stained area, represented as OD/area. The OD/area value was higher in MM bone marrow in contrast with bone marrow from healthy donors (Figure 2B, p<0.001).

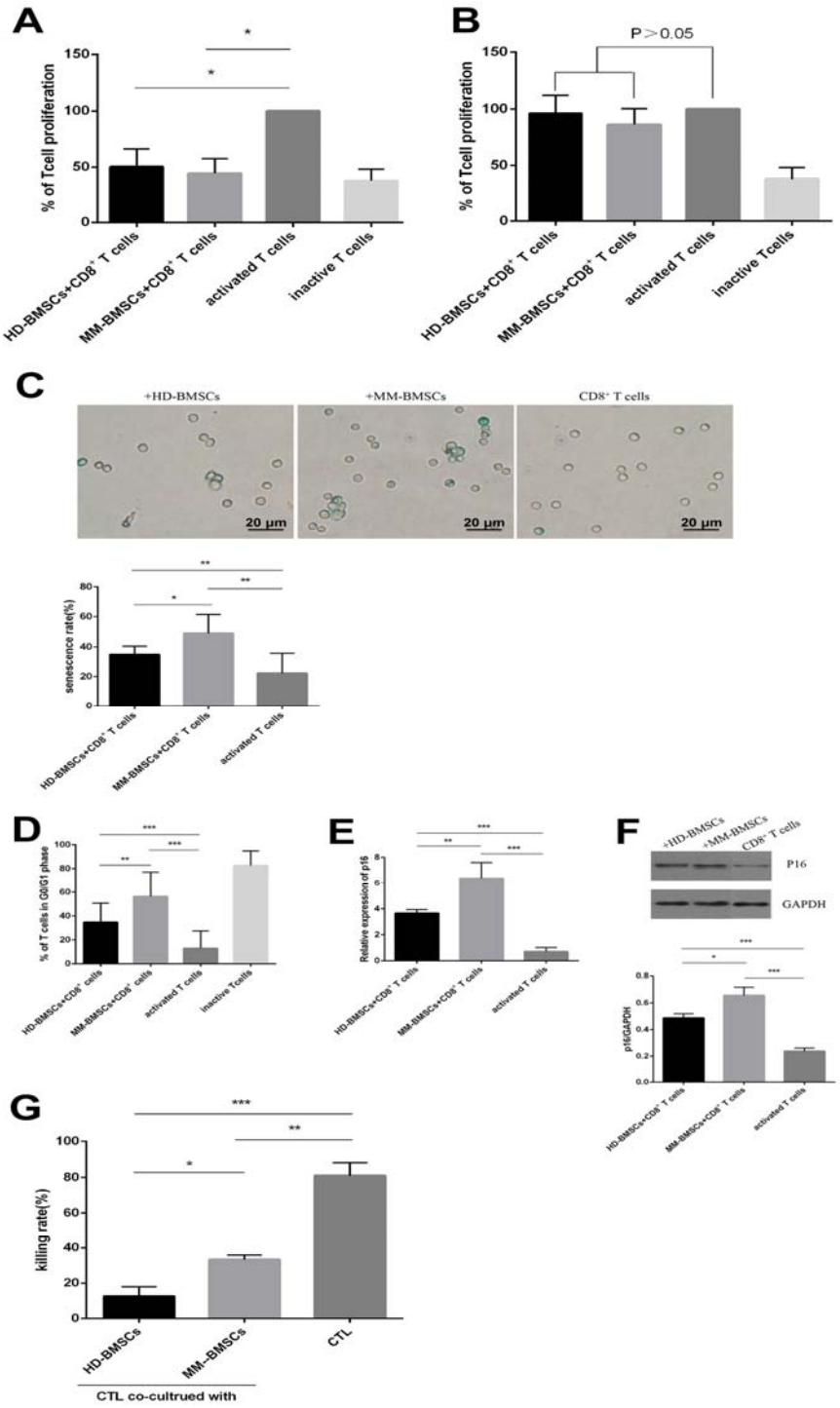

Figure 1. The role of BMSCs on CD8$^+$ T cells. (A) Percentage of proliferative CD8+ T cell in the co-cultured cell-cell groups with HD- or MM-BMSCs (5:1) tested by CCK-8 kit compared to a 100% T-cell proliferation without BMSCs (n=5). (B) Percentage of proliferative CD8+ T cell in the in transwell groups. (C) Percentage of senescent CD8$^+$ T cells co-cultured with or without HD-/MM-BMSCs stained with SA-βgal kit (n=5). (D) Percentage of CD8$^+$ T cells in G0/G1 phase co-cultured with or without HD-/MM-BMSCs analyzed by FCM (n=5). (E) Relative expression of p16 mRNA in CD8$^+$ T cells co-cultured with or without HD-/MM-BMSCs. All cells were analyzed by PCR (n=5). (F). Relative expression of p16 protein in CD8$^+$ T cells co-cultured with or without HD-/MM-BMSCs analyzed by western blot. (G). Tumor specific cytotoxicity of CTL co-cultured with or without HD-/MM-BMSCs (n=5). The killing activity was detected by cck-8 kit. *p<0.05, **p< 0.01, ***p<0.001.

Inhibiting FAPα rescued the proliferation of CD8$^+$ T cells.

As FAPα is involved in immunosuppression of CD4$^+$ T cells (14), we further investigated the role of FAPα in CD8$^+$ T cell immune modulation. 1 pmol/mL and 0.1 pmol/mL PT-100 stimulated the proliferation of CD8$^+$ T cells co-cultured with MM-BMSCs (Figure 3A, $p<0.001$, $p=0.005$, respectively). PT-100 showed a similar effect in the HD-BMSCs group (Figure 3A, $p=0.003$, $p=0.001$, respectively).

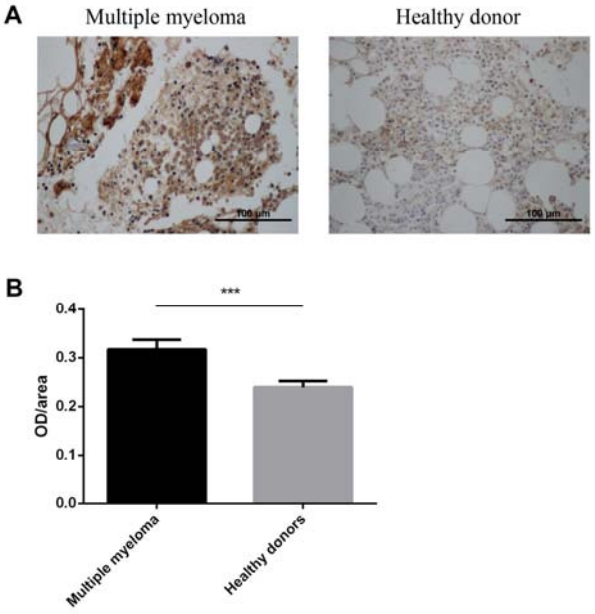

Figure 2. The expression of FAPα in bone marrow. (A) The expression of FAPα in bone marrow mesenchymal matrix was detected by immunohistochemical staining. (B) Quantitative expression of FAPα analyzed by Image-pro plus 6.0, represented in OD/area (n=4). ***p<0.001.

Inhibiting FAPα rescued senescent CD8$^+$ T cells.

To investigate whether the action of BMSCs on CD8$^+$ T cells was related to FAPα expression we investigated the effect of the FAPα inhibitor PT-100. PT-100 weakened MM-BMSCs ability to induce senescence in CD8$^+$ T cells. A significant effect was seen on senescent T cells was observed when MM-BMSCs were treated with 1 pmol/mL and 0.1 pmol/mL PT-100 (Figure 3B, 26.5 ± 6.3%, 36.0 ± 8.9%, $p<0.001$, $p=0.02$, respectively). However, PT-100 did not affect the senescent rate in the HD-BMSCs co-culture group (Figure 3B, $p>0.05$).

Inhibiting FAPα reversed the abnormal G0/G1 phase CD8$^+$ T cell and p16 expression.

We then investigated the role of FAPα in cell cycle arrest using PT-100. The number of CD8$^+$ T cells arrested in G0/G1 phase were decreased to 29.4 ± 17.95% when MM-BMSCs were treated with 1 pmol/mL and 0.1 pmol/mL PT-100 (Figure 3C, $p=0.002$, $p=0.004$, respectively). In addition, 1 pmol/mL and 0.1 pmol/mL PT-100 also reduced p16 mRNA expression dramatically (Figure 3D, $p<0.001$). At protein level, 1 pmol/mL PT-100 down-regulated the p16 expression in MM-BMSCs co-cultured CD8$^+$ T cells from 0.66 ± 0.03 to 0.43 ± 0.04 (Figure 3E, $p=0.009$), we observed a similar change in HD-BMSCs co-cultured CD8$^+$ T cells (Figure 3E, $p<0.01$).

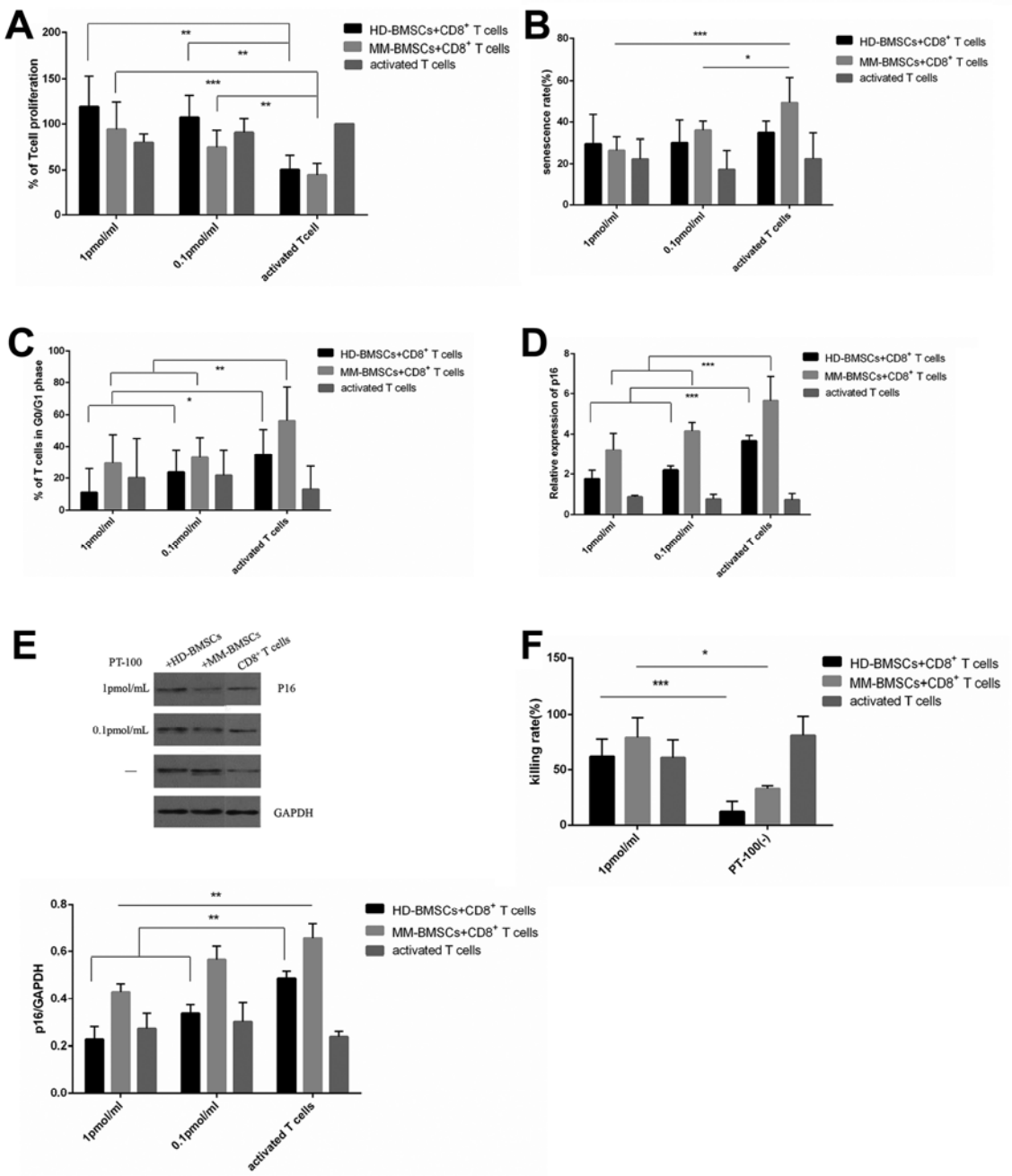

Figure 3. BMSCs exert immunosuppression through FAPα. (A) Percentage of proliferative $CD8^+$ T cell co-cultured with HD- or MM-BMSCs (5:1), which were treated with the FAPα inhibitor PT-100 or not. All cells were tested with aCCK-8 kit (n=5). (B) Percentage of senescent $CD8^+$ T cells (n=5). (C) Percentage of $CD8^+$ T cells in G0/G1 phase analyzed by FCM (n=5). (D) Relative expression of p16 mRNA in $CD8^+$ T cells analyzed by PCR (n=5). (E) Relative expression of p16 protein in CD8+ T cells analyzed by western blot. (F) Tumor specific cytotoxicity of CTL detected with aCCK-8 kit (n=5). *p<0.05, **p<0.01, ***p<0.001.

As senescent T cells are characterized by cell cycle arrest and p16 increase, we inferred that FAPα expressed by MM-BMSCs was associated with $CD8^+$ T cell senescence.

Inhibiting FAPα activated tumor specific cytotoxicity.
We then investigated the role of FAPα on tumor specific cytotoxicity. 1 pmol/mL PT-100 significantly promoted MM-BMSC impaired cytotoxicity (Figure 3F, p=0.043) from 33.32 ± 2.58% to 79.01 ± 18.14%, and we observed similar differences in HD-BMSC co-cultured $CD8^+$ T cells (Figure 3F, p<0.001). The immunosuppression effect of MM-BMSCS is different from HD-BMSCs, MM-BMSCs showed significant $CD8^+$ T cell senescence induction, and this negative effect was mediated by FAPα.

DISCUSSION

Our study focused on the immunomodulatory functions of MM-BMSCs on $CD8^+$ T cell proliferation, senescence, and cytotoxicity. We also identified FAPα was mainly expressed in the mesenchymal matrix in MM biopsy specimens. In addition, we demonstrated that immunosuppression might involve FAPα in a cell-cell dependent manner, indicating that inhibiting FAPα is a potential candidate for future therapeutic applications. Mesenchymal stem cells (MSCs) have been suggested to affect T-cell proliferation through both cell contact-dependent and independent mechanisms (25). Our results suggest that in this case MM-BMSCs exert immunosuppression in a cell-cell dependent manner, as no notable differences of proliferative rate was observed during transwell co-culture. This study did not investigate the details of the cell-cell dependent mechanism, but previous studies suggest complex cytoskeletal structures may be involved. Tunneling nanotubes (TNTs), a novel mode of cell communication, are trans-membrane constructions that facilitate the transport of several types of cargo, including organelles, pathogens, calcium fluxes, death signals, and membrane-bound proteins (26-29). TNTs have been found between adjacent BMSCs and H9c2 cells and rescued apoptotic H9c2 cells (30). We suggest that formation of these cytoskeletal structures between MM-BMSCs and $CD8^+$ T cells, is a possible mediator of MM-BMSCs immunosuppression. Previous study has documented that HD-BMSCs are capable of inhibiting proliferation, promoting apoptosis, arresting the cell cycle and preventing activation of T cells; however, these immunosuppression functions are dysfunctional in MM-BMSCs (10). While the CCK-8 assay suggested that the inhibitory function of BMSCs was independent of their source, we also found notably that $CD8^+$ T cell senescence, cycle arrest and increased p16 expression occurred with MM-BMSC co-culture, suggesting that MM-BMSCs exert an immunosuppression effect by promoting T cell senescence. Accumulation of senescent T-cells has been found in patients with chronic viral infections and with particular types of cancers, suggesting that different types of human cancer cells and Treg cells can induce T-cell senescence (15,16,31). Cell cycle controlling proteins such as p16 normally inhibit cell cycle progression and have been shown to accumulate in senescent cells with defective cytotoxicity and negative regulatory functions (32,33). MM-BMSCs mainly up-regulated p16 expression and induced $CD8^+$ T cell cycle arrest, resulting in T cell exhaustion, on the other hand, HD-BMSCs mainly increased apoptosis (10), thus we observed that HD-BMSCs inhibited cytotoxicity dramatically compared to MM-BMSCs. FAPα expressing cells, mostly cancer associated fibroblasts, in tumor microenvironments have been shown to produce TGF-β, IL-10, IL-4 and platelet derived growth factor (PDGF) which are associated with immunosuppressive T cell production (34). Tumor growth can be controlled by depleting FAP^+ cells in an adaptive immunity-dependent manner, so this

suggests that FAPα is responsible for $CD8^+$ T-cell anergy, where the lymphocyte is functionally inactivated following an antigen encounter. When treated with the FAPα inhibitor, PT-100, $CD8^+$ T cells showed restored proliferation and tumor specific cytotoxicity, and only rescued the senescent $CD8^+$ T cells stimulated by MM-BMSCs. FAPα expressed by MM-BMSCs mediated protection of bortezomib-induced MM cell lines apoptosis and this protection effect may likely through β-catenin pathway (23). T-cell factor (TCF-1) is the effector transcription factor of the WNT signaling pathway. It has been confirmed that Wnt/β-catenin signaling and TCF-1 are highly activated and expressed in undifferentiated $CD8^+$ T and memory $CD8^+$ T cells and that TCF-1 is down-regulated when naive $CD8^+$ T cells differentiate into effector $CD8^+$ T cells (35). In addition, Wnt/β-catenin signaling diminishes priming and infiltrating of CTL (36). Tumor microenvironment of metastatic melanoma and other cancer types prefer to activate Wnt/β-catenin signaling, which is associated with exhaustion of T cells (37). FAPα in MM microenvironment might markedly activate Wnt/β-catenin signaling, leading to the loss of effector $CD8^+$ T cells and accumulation of senescent $CD8^+$ T cells. This theory would be the possible way to explain how PT-100 only down-regulated senescent $CD8^+$ T cells co-cultured with MM-BMSCs. The mechanisms are needed to be further illuminated. Taken together, the results of this study suggest that MM-BMSCs exert their immunosuppressive effect, through the induction of senescence, on $CD8^+$ T cells. This effect may be associated with FAPα expressed by BMSCs, providing a potential target for more successful MM immunotherapy.

ACKNOWLEDGEMENTS

This study was supported by grants from the National Natural Science Foundation of China (81201866) and the Specialized Research Fund for the Doctoral Program of Higher Education of China (20120142120077).

REFERENCES

1. Rajkumar SV. Multiple myeloma: 2016 update on diagnosis, risk-stratification, and management. Am J Hematol. 2016; 91:719-734.
2. Landgren O, Rajkumar SV. New Developments in Diagnosis, Prognosis, and Assessment of Response in Multiple Myeloma. Clin Cancer Res. 2016; 22:5428-5433.
3. Siegel R. Iron deficiency anaemia and rectal bleeding - advanced haemorrhoidal disease. MMW Fortschr Med. 2018; 160:48-50.
4. Ayed AO, Chang LJ, Moreb JS. Immunotherapy for multiple myeloma: Current status and future directions. Crit Rev Oncol Hematol. 2015; 96:399-412.
5. Castells M, Thibault B, Delord JP, Couderc B. Implication of tumor microenvironment in chemoresistance: tumor-associated stromal cells protect tumor cells from cell death. Int J Mol Sci. 2012; 13:9545-9571.
6. Raz Y, Erez N. An inflammatory vicious cycle: Fibroblasts and immune cell recruitment in cancer. Exp Cell Res. 2013; 319:1596-1603.
7. Servais C, Erez N. From sentinel cells to inflammatory culprits: cancer-associated fibroblasts in tumour-related inflammation. J Pathol. 2013; 229:198-207.
8. Fu Z, Zuo Y, Li D, Xu W, Li D, Chen H, et al. The crosstalk: Tumor-infiltrating lymphocytes rich in regulatory T cells suppressed cancer-associated fibroblasts. Acta Oncol. 2013; 52:1760-1770.

9. Spaeth EL, Dembinski JL, Sasser AK, Watson K, Klopp A, Hall B, et al. Mesenchymal stem cell transition to tumor-associated fibroblasts contributes to fibrovascular network expansion and tumor progression. PLoS One. 2009; 4:e4992.
10. Andre T, Najar M, Stamatopoulos B, Pieters K, Pradier O, Bron D, et al. Immune impairments in multiple myeloma bone marrow mesenchymal stromal cells. Cancer Immunol Immunother. 2015; 64:213-224.
11. Meisel R, Zibert A, Laryea M, Gobel U, Daubener W, Dilloo D. Human bone marrow stromal cells inhibit allogeneic T-cell responses by indoleamine 2,3-dioxygenase-mediated tryptophan degradation. Blood. 2004; 103:4619-4621.
12. Kong QF, Sun B, Wang GY, Zhai DX, Mu LL, Wang DD, et al. BM stromal cells ameliorate experimental autoimmune myasthenia gravis by altering the balance of Th cells through the secretion of IDO. Eur J Immunol. 2009; 39:800-809.
13. Castro-Manrreza ME, Mayani H, Monroy-Garcia A, Flores-Figueroa E, Chavez-Rueda K, Legorreta-Haquet V, et al. Human mesenchymal stromal cells from adult and neonatal sources: a comparative in vitro analysis of their immunosuppressive properties against T cells. Stem Cells Dev. 2014; 23:1217-1232.
14. Wu X, Wang Y, Xu J, Luo T, Deng J, Hu Y. MM-BMSCs induce naive CD4+ T lymphocytes dysfunction through fibroblast activation protein alpha. Oncotarget. 2017; 8:52614-52628.
15. Tsukishiro T, Donnenberg AD, Whiteside TL. Rapid turnover of the CD8(+)CD28(-) T-cell subset of effector cells in the circulation of patients with head and neck cancer. Cancer Immunol Immunother. 2003; 52:599-607.
16. Mondal AM, Horikawa I, Pine SR, Fujita K, Morgan KM, Vera E, et al. p53 isoforms regulate aging- and tumor-associated replicative senescence in T lymphocytes. J Clin Invest. 2013; 123:5247-5257.
17. Nelson JA, Krishnamurthy J, Menezes P, Liu Y, Hudgens MG, Sharpless NE, et al. Expression of p16(INK4a) as a biomarker of T-cell aging in HIV-infected patients prior to and during antiretroviral therapy. Aging Cell. 2012; 11:916-918.
18. Migliaccio M, Alves PM, Romero P, Rufer N. Distinct mechanisms control human naive and antigen-experienced CD8+ T lymphocyte proliferation. J Immunol. 2006; 176:2173-2182.
19. Nasi M, Pinti M, De Biasi S, Gibellini L, Ferraro D, Mussini C, et al. Aging with HIV infection: a journey to the center of inflammAIDS, immunosenescence and neuroHIV. Immunol Lett. 2014; 162:329-333.
20. Garin-Chesa P, Old LJ, Rettig WJ. Cell surface glycoprotein of reactive stromal fibroblasts as a potential antibody target in human epithelial cancers. Proc Natl Acad Sci U S A. 1990; 87:7235-7239.
21. Busek P, Balaziova E, Matrasova I, Hilser M, Tomas R, Syrucek M, et al. Fibroblast activation protein alpha is expressed by transformed and stromal cells and is associated with mesenchymal features in glioblastoma. Tumour Biol. 2016; 37:13961-13971.
22. Cohen SJ, Alpaugh RK, Palazzo I, Meropol NJ, Rogatko A, Xu Z, et al. Fibroblast activation protein and its relationship to clinical outcome in pancreatic adenocarcinoma. Pancreas. 2008; 37:154-158.
23. Zi FM, He JS, Li Y, Wu C, Wu WJ, Yang Y, et al. Fibroblast activation protein protects bortezomib-induced apoptosis in multiple myeloma cells through beta-catenin signaling pathway. Cancer Biol Ther. 2014; 15:1413-1422.
24. Kraman M, Bambrough PJ, Arnold JN, Roberts EW, Magiera L, Jones JO, et al. Suppression of antitumor immunity by stromal cells expressing fibroblast activation protein-alpha. Science. 2010; 330:827-830.
25. Benvenuto F, Voci A, Carminati E, Gualandi F, Mancardi G, Uccelli A, et al. Human mesenchymal stem cells target adhesion molecules and receptors involved in T cell extravasation. Stem Cell Res Ther. 2015; 6:245.
26. Rainy N, Chetrit D, Rouger V, Vernitsky H, Rechavi O, Marguet D, et al. H-Ras transfers from B to T cells via tunneling nanotubes. Cell Death Dis. 2013; 4:e726.
27. Watkins SC, Salter RD. Functional connectivity between immune cells mediated by tunneling nanotubules. Immunity. 2005; 23:309-318.

28. Arkwright PD, Luchetti F, Tour J, Roberts C, Ayub R, Morales AP, et al. Fas stimulation of T lymphocytes promotes rapid intercellular exchange of death signals via membrane nanotubes. Cell Res. 2010; 20:72-88.
29. Pasquier J, Galas L, Boulange-Lecomte C, Rioult D, Bultelle F, Magal P, et al. Different modalities of intercellular membrane exchanges mediate cell-to-cell p-glycoprotein transfers in MCF-7 breast cancer cells. J Biol Chem. 2012; 287:7374-7387.
30. Han H, Hu J, Yan Q, Zhu J, Zhu Z, Chen Y, et al. Bone marrow-derived mesenchymal stem cells rescue injured H9c2 cells via transferring intact mitochondria through tunneling nanotubes in an in vitro simulated ischemia/reperfusion model. Mol Med Rep. 2016; 13:1517-1524.
31. Weng NP, Akbar AN, Goronzy J. CD28(-) T cells: their role in the age-associated decline of immune function. Trends Immunol. 2009; 30:306-312.
32. Beausejour CM, Krtolica A, Galimi F, Narita M, Lowe SW, Yaswen P, et al. Reversal of human cellular senescence: roles of the p53 and p16 pathways. EMBO J. 2003; 22:4212-4222.
33. Akbar AN, Henson SM. Are senescence and exhaustion intertwined or unrelated processes that compromise immunity? Nat Rev Immunol. 2011; 11:289-295.
34. Vasievich EA, Huang L. The suppressive tumor microenvironment: a challenge in cancer immunotherapy. Mol Pharm. 2011; 8:635-641.
35. Gattinoni L, Zhong XS, Palmer DC, Ji Y, Hinrichs CS, Yu Z, Wrzesinski C, Boni A, Cassard L, Garvin LM, Paulos CM, Muranski P, Restifo NP. Wnt signaling arrests effector T cell differentiation and generates CD8+ memory stem cells. Nat Med. 2009; 15:808-13.
36. Yaguchi T, Goto Y, Kido K, Mochimaru H, Sakurai T, Tsukamoto N, et al. Immune suppression and resistance mediated by constitutive activation of Wnt/beta-catenin signaling in human melanoma cells. J Immunol 2012; 189:2110–7.
37. Trujillo JA, Sweis RA-O, Bao R, Luke JJ. T cell-inflamed versus non-T cell-inflamed tumors: a conceptual framework for cancer immunotherapydrug development and combination therapy selection. Cancer Immunol Res. 2018; 6:990–1000.